# How to exploit the features of microfluidics technology

DOI: 10.1039/b717986n

## Introduction

In recent years, microfluidics technology has enabled the genesis of novel and commercially successful products ranging from portable insulin delivery devices[1] to high speed inkjet printers.[2] However, during this period of rapid technological evolution, it is important to recognize that microfluidics is an enabling technological tool that can potentially provide increased functionality compared to systems that utilize conventional, "macroscale" methods. While it may seem somewhat obvious, it is also important to realize that, like all tools, microfluidics can be particularly powerful for certain applications and not advantageous for others. For example, microfluidics may be especially well suited for applications that require handing of small amounts of samples (*e.g.* single cell analysis), conversely, it may be inappropriate for applications that require high volumetric throughputs (*e.g.* sewage treatment plants). Thus, when designing microfluidic devices, it is important not to simply scale down macroscopic processes to the microscale. Instead, it is prudent to understand and exploit the relevant physics and chemistries at the smaller length scales. Toward this end, the aim of this Focus article is to highlight a few characteristics of microfluidics technology which we think are particularly useful and provide examples of applications that exploit them. For the purposes of this article, we define microfluidics as the *methodology and/or mechanism for controlled transport of measurable quantities, such as mass, energy and momentum, in a microscale environment*. The word "control" is judiciously chosen, because we believe that it embodies the crux of microfluidics technology. In the following sections, we will focus our discussions on the effects of high surface area to volume ratio, and the utility of accurately controlling force fields within microfluidic devices.

## Effects of high surface area to volume ratios

One characteristic of microscale and nanoscale devices is the high surface area to volume ratio (SAV), and this characteristic can lead to unconventional overriding forces. For example, large SAVs typically make surface forces (such as surface tension) the dominant force, while greatly reducing the influence of inertial and body forces. An example of a microfluidic architecture that takes advantage of this feature involves "digital microfluidic technology" where droplets of water/oil are created and transported in a controlled fashion to achieve functions such as storage, mixing, chemical reaction, or analysis, in a discrete manner.[4,5] The droplets are formed using the surface tension properties of liquid, as well as by controlling the hydrophobicity of the substrate *via* electrical fields and/or material coating. Digital microfluidics is gaining much attention because of its ability to precisely control transport in the water/oil droplets. This technology currently has the capability of being programmable, reconfigurable, and reusable, towards the goal of creating a lab-on-a-chip.[6]

High SAV is also advantageous for on-chip microfluidic capillary electrophoresis (CE) devices. On-chip microfluidic CE devices were first described in the late 1980s by several pioneering researchers.[7–9] With the on-chip format, there is a higher SAV than traditional, macroscale CE systems, which allows for greater dissipation of the Joule heating that is usually generated from the application of high electric fields. Joule heating within CE systems leads to the detrimental effect of nonlinear flow, excessive heat dissipation and faradaic reactions. Therefore, minimization of Joule heating allows for increased performance, higher sensitivity and increased resolution of separations, and allows the separation of compounds that have been traditionally difficult to handle by both HPLC and traditional CE instruments.[10,11]

A final compelling example of how large SAV can be exploited in microfluidic devices is shown in a recent work by Piorek and coworkers to automatically capture airborne molecules in a free-surface micofluidic architecture.[12,13] In this system, the microchannel is 1.5 microns deep by 15 microns wide, and the top of the channel is open and exposed to the surrounding atmosphere. The free fluidic surface is confined by surface tension and generates a pressure gradient-driven flow, and the large SAV allows water-soluble airborne molecules to absorb into the channel, without being significantly diluted into a large volume of fluid. Once absorbed into the channel, the molecules adsorb onto Ag nanoparticles. The interaction of the molecules with the Ag nanoparticles initiates a 'controlled' aggregation process that produces SERS-active dimers that cause a $10^{10}$–$10^{12}$ amplification of Raman signal. The Surface-Enhanced Raman Spectroscopy (SERS) signal can then be analyzed to determine the molecule type. In the particular example shown in Fig. 1, a large SAV is utilized in a variety of ways to (1) drive the flow using capillary effects and surface tension, (2) create a large free surface to adsorb airborne molecules, (3) minimize dilution into the bulk fluid, and (4) control nanoparticle aggregation dynamics.

Although high SAV can be extremely advantageous, it can also be detrimental. For example, in microfluidic CE, molecules can be more readily adsorbed onto the surfaces of the microchannel than in more traditional systems, thereby decreasing the efficiency of transport. Although there has been much research to mitigate this problem,[14] microfluidics is not the ideal tool to use when surface fouling may be a concern.

## Accurate control of force fields

Many groups have documented the unique and sometimes counterintuitive flow of liquids in microfluidic channels in recent articles.[11,15,16] Among others,

 

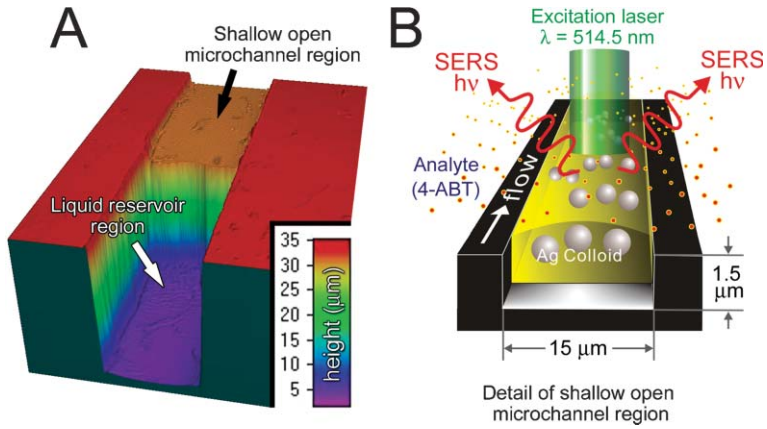


**Fig. 1** Microfluidic/SERS sensing device. The device is designed for free surface fluidics and is easily coupled with SERS detection: (A) Three-dimensional profile of the microfluidic device showing the transition from the 30 μm deep fluid reservoir to the open 1.5 μm deep microchannel section. The flow channels are 15 μm wide and were characterized with 3-D confocal microscopy (HS 200A Advanced Confocal Optical Profiler; Hyphenated Systems, Burlingame, CA, USA). (B) Schematic of microfluidic sensor for analysis of gas-phase species. The free-surface liquid/atmosphere interface allows analyte absorption and subsequent optical stimulation with a $\lambda$ = 514.5 nm laser for SERS detection. [Reproduced from Piorek *et al.*,[12] with permission.]

perhaps the most important phenomenon at the microscale is that viscous and body forces dominate over inertial and pressure forces. This leads to well-defined flow characteristics, such as perfect fore–aft symmetry of fluid flow and laminar flow.[11] In addition, when we apply external body forces, such as electric or magnetic fields, we can further control the fluid flow because the applied fields can be engineered accurately. Such characteristics of microfluidics can be advantageous when one wants to precisely define the velocity fields and the location of particles and reagents in a system. Examples of microfluidic systems that exploit this are electro thermal stirring devices,[17–20] and high performance cell sorting.[21,22]

Using AC-driven electrothermal flow (ETF) to enhance the performance of immuno-sensors is one application that exploits the capability to precise control electric fields. ETF generates a circular stirring motion in a fluid that increases the interactions between surface immobilized molecules with those in suspension (see Fig. 2). ETF results from a conductivity gradient produced by localized Joule heating, which interacts with an applied AC electric field. ETF is effective in higher conductivity solutions and can be useful for biological assays to accelerate the time required to operate diffusion-limited reactions, which is important for both field-portable sensors and for lab-based microarray assays.

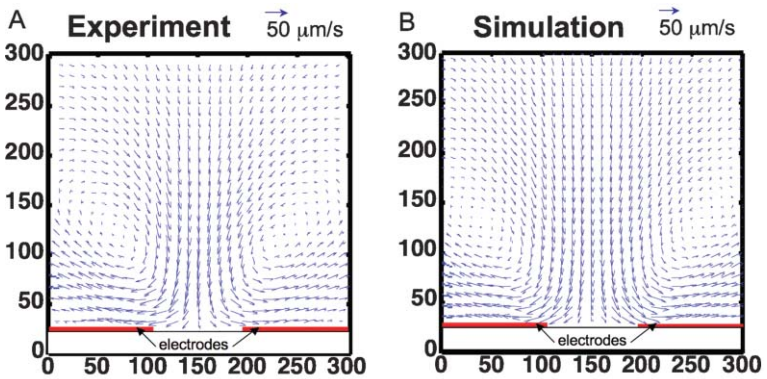


**Fig. 2** Velocity field of electrothermal flow (ETF) comparing experiments to simulation. A. Fluid velocity field measured in electrothermal test device. B. Numerical model of ETF. The circulating flow pattern matches well with the experimentally-measured velocity.[17]

Another interesting area where microfluidics and controlled force fields play an important role is in high-performance cell sorting. The performance of cell separation is typically characterized by three metrics: "throughput" gauges how many cell sorting operations can be executed per unit of time, "purity" is the fraction of the target cells in the collection vessel, and "recovery" is the fraction of the input target cells successfully sorted into the collection vessel. In conventional technologies such as Fluorescence Activated Cell Sorters (FACS) and Magnetic Activated Cell Sorters (MACS), the current challenges arise from the fact that the three performance metrics are coupled, such that increasing one parameter usually comes at the expense of another (*e.g.*, high throughput usually comes at a cost of purity *etc.*). Microfluidics technology provides an alternate strategy to decouple these parameters by allowing integrated devices to operate in parallel. Furthermore, microfluidics technology offers the potential to provide disposable solutions, thereby eliminating sample cross-contamination.

Among the many methods of cell sorting in microfluidic devices, a significant number of research groups have exploited the phenomenon of dielectrophoresis[23] to manipulate particles ranging from beads, viruses, bacteria, and mammalian cells.[22,24–27] Dielectrophoresis refers to the force resulting from differences in dielectric properties between a particle and its surrounding medium in a spatially varying electric field. One of the major advantages of this phenomenon is that the polarity of the force (attraction or repulsion) can be controlled with the frequency of the applied voltage. In addition, this force is particularly well suited for microfluidics because microfabrication processes allow precise patterning of miniaturized electrodes such that the non-uniform electric fields, and thus, the resulting dielectrophoretic force fields, can be created with extraordinary accuracy and reproducibility which cannot be implemented in conventional, macroscopic technologies. Such capabilities have allowed the development of novel cell sorting architectures including those that integrate multiple cell sorting stages on to a single monolithic chip to

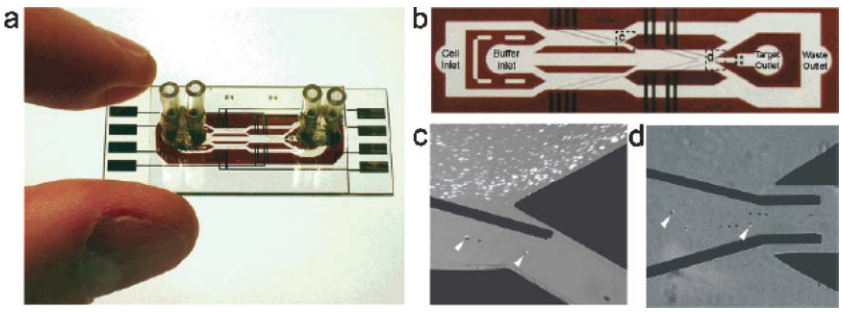


**Fig. 3** A Two-stage Dielectrophoresis Activated Cell Sorter (DACS) device. (A) Photograph of the device; it is fabricated with glass substrates and a polyimide layer (red areas) that defines the fluid channels (white areas). (B) Top view of the device showing the angled deflector electrodes. (C) Micrograph of the DACS device in operation showing the first sorting stage. Laminar fluid flow (from left to right) prevents mixing of the buffer and sample streams. Target cells labeled with beads (shown with arrows) are dielectrophoretically deflected into the buffer stream toward the second purification stage, whereas the non-target cells elute to the waste channel without being deflected. (D) Micrograph of the second stage at the collection outlet. The integration of tandem purification stages significantly increases the purity of the target cells. [Taken from Bessette *et al.*,[3] with permission.]

significantly increase the purity and recovery performance over those of macro-scale devices (as shown in Fig. 3). The availability of such high purity, disposable microfluidic cell sorters are beginning to open new directions in the area of high throughput molecular screening[3] and integrated *in vitro* diagnostics (IVD).

Note that although laminar flow and control of flow fields are advantageous in many situations, the lack of inertia can be disadvantageous when trying to develop a device that requires rapid mixing. In the absence of inertia and diffusion, particles will not cross fluid streamlines, and will not mix. In many situations mixing results purely from molecular diffusion. Diffusion limited mixing is simple and controlled, but can be very slow, and in many situations inadequate. Therefore, researchers have established mixing by utilizing electrokinetic instabilities,[28] chaotic advection,[29] and microstirring.[30] In general, however, microfluidics may not be the optimum tool for fluid mixing, and readers may want to instead explore off-chip sample preparation devices and components currently being developed.[31]

## Summary

In summary, microfluidics technology is a useful tool that has, and will continue to, enable new fluidic functions for a wide range of applications. In addition to the characteristics that we discussed above, it is obvious that the small size inherent to microfluidics can potentially enable portability, reduced reagent consumption, reduced analysis time, and increased efficiency. It is our intent to illustrate some advantages and disadvantages of microfluidic technology which often occur simultaneously and in conflict. These apparent contradictions may lead to technical insights that can move the research community forward.

**S. Pennathur**
Department of Mechanical Engineering, University of California, Santa Barbara, USA
sumita@engineering.ucsb.edu
**C. D. Meinhart**
Department of Mechanical Engineering, University of California, Santa Barbara, USA
**H. T. Soh**
Department of Materials and Mechanical Engineering, University of California, Santa Barbara, USA

## References

1 T. Kubik, K. Bogunia-Kubik and M. Sugisaka, *Curr. Pharm. Biotechnol.*, 2005, **6**, 17–33.
2 J. Chen and K. D. Wise, in *Proceedings of the International Conference on Solid-State Sensors and Actuators, and Eurosensors IX*, 1995, vol. 2, pp. 321–324.
3 P. H. Bessette, X. Hu, H. T. Soh and P. S. Daugherty, *Anal. Chem.*, 2007, **79**, 2174–2178.
4 D. R. Link, E. Grasland-Mongrain, A. Duri, F. Sarrazin, Z. Cheng, G. Cristobal, M. Marquez and D. A. Weitz, *Angew. Chem., Int. Ed.*, 2006, **45**, 2556–2560.
5 A. S. Utada, L.-Y. Chu, A. Fernandez-Nieves, D. R. Link, C. Holtze and D. A. Weitz, *MRS Bull.*, 2007, **32**, 702–708.
6 R. B. Fair, *Microfluid. Nanofluid.*, 2007, **3**, 245–281.
7 G. H. W. Sanders and A. Manz, *TrAC, Trends Anal. Chem.*, 2000, **19**, 364–378.
8 R. D. Oleschuk, L. L. Shultz-Lockyear, Y. Ning and D. J. Harrison, *Anal. Chem.*, 2000, **72**, 585–590.
9 S. C. Jacobson, A. W. Moore and J. M. Ramsey, *Anal. Chem.*, 1995, **67**, 2059–2063.
10 D. J. Beebe, G. A. Mensing and G. M. Walker, *Annu. Rev. Biomed. Eng.*, 2002, **4**, 261–286.
11 T. M. Squires and S. R. Quake, *Rev. Mod. Phys.*, 2005, **77**, 977–1026.
12 B. D. Piorek, S.-J. Lee, J. G. Santiago, M. Moskovits, S. Banerjee and C. D. Meinhart, *Proc. Natl. Acad. Sci. U. S. A.*, 2007, **108**(48), 18898–18907.
13 B. Piorek, A. Mechler, R. Lal, P. Freudenthal, C. Meinhart and S. Banerjee, *Appl. Phys. Lett.*, 2006, 89.
14 L. Kim, Y.-C. Toh, J. Voldman and H. Yu, *Lab Chip*, 2007, **7**, 681–694.
15 J. M. Ramsey, *Nat. Biotechnol.*, 1999, **17**, 1061–1062.
16 E. M. Purcell, *Am. J. Phys.*, 1977, **45**, 3–11.
17 M. Sigurdson, D. Wang and C. D. Meinhart, *Lab Chip*, 2005, **5**, 1366–1373.
18 C.-K. Yang, J.-S. Chang, S. D. Chao and K.-C. Wu, *Appl. Phys. Lett.*, 2007, 91.
19 J. Wu, M. Lian and K. Yang, *Appl. Phys. Lett.*, 2007, 90.
20 G. Hu, Y. Gao and D. Li, *Biosens. Bioelectron.*, 2007, **22**, 1403–1409.
21 M. M. Wang, E. Tu, D. E. Raymond, J. M. Yang, H. Zhang, N. Hagen, B. Dees, E. M. Mercer, A. H. Forster, I. Kariv, P. J. Marchand and W. F. Butler, *Nat. Biotechnol.*, 2005, **23**, 83–87.
22 X. Hu, P. H. Bessette, J. Qian, C. D. Meinhart, P. S. Daugherty and H. T. Soh, *Proc. Natl. Acad. Sci. U. S. A.*, 2005, **102**, 15757–15761.
23 H. Pohl, *Dielectrophoresis: The Behavior of Neutral Nonuniform Electric Fields*, Cambridge University Press, Cambridge, UK, 1978.
24 U. Seger, S. Gawad, R. Johann, A. Bertsch and P. Renaud, *Lab Chip*, 2004, **4**, 148–151.
25 P. R. C. Gascoyne and J. Vykoukal, *Electrophoresis*, 2002, **23**, 1973–1983.
26 J. G. Kralj, M. T. W. Lis, M. A. Schmidt and K. F. Jensen, *Anal. Chem.*, 2006, **78**, 5019–5025.
27 S. Fiedler, S. G. Shirley, T. Schnelle and G. Fuhr, *Anal. Chem.*, 1998, **70**, 1909–1915.
28 H. Lin, B. D. Storey, M. H. Oddy, C.-H. Chen and J. G. Santiago, *Phys. Fluids*, 2004, **16**, 1922–1935.
29 H. Aref, *J. Fluid Mech.*, 1984, **143**, 1–21.
30 M. Heule and A. Manz, *Lab Chip*, 2004, **4**, 506–511.
31 G. Chirica, J. Lachmann and J. Chan, *Anal. Chem.*, 2006, **78**, 5362–5368.

 